



Published in final edited form as:

*J Neurochem.* 2016 July ; 138(2): 354–361. doi:10.1111/jnc.13650.

## Role of serum- and glucocorticoid-inducible kinases in stroke

Koichi Inoue<sup>1,2,\*</sup>, Tiandong Leng<sup>1</sup>, Tao Yang<sup>1</sup>, Zhao Zeng<sup>1</sup>, Takatoshi Ueki<sup>2</sup>, and Zhi-Gang Xiong<sup>1</sup>

<sup>1</sup>Neuroscience Institute, Morehouse School of Medicine, Atlanta, Georgia 30310, USA

<sup>2</sup>Department of Integrative Anatomy, Nagoya City University Graduate School of Medical Sciences, Nagoya 467-8601, Japan

### Abstract

Increased expression of serum- and glucocorticoid-inducible kinase 1 (SGK1) can be induced by stress and growth factors in mammals, and plays an important role in cancer, diabetes and hypertension. A recent work suggested that SGK1 activity restores damage in a stroke model. To further investigate the role of SGKs in ischemic brain injury, we examined how SGK inhibitors influence stroke outcome *in vivo* and neurotoxicity *in vitro*. Infarct volumes were compared in adult mice with middle cerebral artery occlusion (MCAO), followed by 24 h reperfusion, in the absence or presence of SGK inhibitors. Neurotoxicity assay, electrophysiological recording and fluorescence Ca<sup>2+</sup> imaging were carried out using cultured cortical neurons to evaluate the underlying mechanisms. Contrary to our expectation, infarct volume by stroke decreased significantly when SGK inhibitor, gsk650394 or EMD638683, was administrated 30 min before MCAO under normal and diabetic conditions. SGK inhibitors reduced neurotoxicity mediated by N-methyl-D-aspartate (NMDA) receptors, a leading factor responsible for cell death in stroke. SGK inhibitors also ameliorated Ca<sup>2+</sup> increase and peak amplitude of NMDA current in cultured neurons. In addition, SGK inhibitor gsk650394 decreased phosphorylation of Nedd4-2 and inhibited voltage-gated sodium currents. These observations suggest that SGK activity exacerbates stroke damage and that SGK inhibitors may be useful candidates for therapeutic intervention.

### Keywords

SGK1; stroke; mouse; glutamate; NMDA; sodium channels

### Introduction

Stroke, caused by an interruption of blood supply to the brain, represents one of the leading causes of morbidity and mortality worldwide and often results in permanent neurological disabilities including cognitive impairment and seizures. Despite the long history of effort in the search for effective treatment, tissue plasminogen activator is still the only FDA

\*Correspondence: Neuroscience Institute, Morehouse School of Medicine, 720 Westview Drive SW, Atlanta, Georgia 30310, Phone: 404-756-6698, Fax: 404-752-1041, ino-k@umin.ac.jp.

### Competing financial interests

The authors declare no competing financial interests.

approved agent for stroke (Lo *et al.* 2004). It has a limited therapeutic time window and the potential side effect of intracranial hemorrhage. Therefore, disclosing new targets in stroke may shed new light on future stroke therapy (Lo *et al.* 2004, Gurman *et al.* 2015).

Serum- and glucocorticoid-inducible kinase 1 (SGK1) is a member of the SGK family and is expressed in the brain (Lang *et al.* 2006a). Its expression is rapidly induced by stimuli including serum and glucocorticoid, while other members of SGK, SGK2 and SGK3, are not induced by those stimuli (Lang *et al.* 2006a). Increasing evidence suggests that SGKs including SGK1 contribute to various physiological and pathophysiological processes (Lang *et al.* 2006a, Lang *et al.* 2009). Especially, SGK1 is known to regulate epithelial Na<sup>+</sup> channels (ENaCs), which play a critical role in Na<sup>+</sup> reabsorption in the kidney (Benos *et al.* 1996). Regulation of most channels/transporters such as ENaCs by SGK1 acts through E3 ubiquitin ligase Nedd4-2. Nedd4-2 binds to those channels/transporters and the complex is internalized and degraded. However, when phosphorylated by SGK1, Nedd4-2 does not bind to them and the surface expression levels of those channels/transporters are consequently elevated (Debonneville *et al.* 2001, Lang *et al.* 2006a). Therefore, SGK1 activity influences internal Na<sup>+</sup> accumulation and consequently the level of blood pressure (Wulff *et al.* 2002, Busjahn *et al.* 2002, von Wowern *et al.* 2005).

Considering that SGK1 regulates the activity of ion channels and transporters and that SGK1 influences blood pressure, it is highly likely that SGK1 affects the outcome of stroke. Interestingly, its expression in the human brain tends to increase with ageing as shown by microarray data (Lu *et al.* 2004), suggesting that SGK1 could also play a role in the higher incidence of stroke among elderly individuals. Zhang *et al.* recently reported that overexpressing SGK1 in neurons is protective against ischemic injury *in vitro* and *in vivo* (Zhang *et al.* 2014). This could be conceivable as SGK1 may share downstream targets with anti-apoptotic Akt/PKB signaling (Lang *et al.* 2006a, Lang *et al.* 2010, Wick *et al.* 2002, Gervitz *et al.* 2002, Manning & Cantley 2007). Accordingly, inhibition of SGK1 activity is expected to be detrimental to stroke outcome. In addition to neurons, SGK1 is also expressed and plays a role in glial cells (Miyata *et al.* 2015, Slezak *et al.* 2013). It is interesting to see what occurs when both neuronal and glial SGKs are inhibited in the brain.

There are recently developed SGK inhibitors, gsk650394 and EMD638683, which affect not only SGK1 but also other SGK members (Sherk *et al.* 2008, Ackermann *et al.* 2011). Studying the effects of these agents on stroke outcome could provide important information in regard to human therapeutic strategy for targeting SGKs including SGK1. This study explores the effect of SGK inhibitors on ischemic brain injury *in vivo* and the underlying neuroprotective mechanism *in vitro*.

## Materials and Methods

### Animals

Adult C57BL6 mice (25–30 g, 8–10 weeks old, male) and pregnant Swiss mice were purchased from Charles River. Experiments were conducted in accordance with the Guidelines of Institutional Animal Care and Use Committee of Morehouse School of Medicine.

### Diabetic models

Type I diabetic mice were created as described previously (Federiuk *et al.* 2004). Briefly, alloxan (80 to 100 mg/kg) was injected intravenously into mice to chemically destroy Langerhans  $\beta$ -cells of pancreases. After a week, blood glucose levels were tested, and mice were regarded as diabetic if the fasting blood glucose concentration was over 15 mM (270 mg/dl).

### Stroke models

Transient focal ischemia was induced by suture occlusion of the middle cerebral artery (MCAO) for 1 h (under normal condition) or 45 min (under diabetic condition) as described previously (Xiong *et al.* 2004, Pignataro *et al.* 2008). gsk650394 (Santa Cruz) and EMD638683 (Chemescene) were first dissolved in dimethylsulfoxide (DMSO) at 10 mM. They were then diluted 10-times in saline to make a working solution at 1 mM for injection (1  $\mu$ l). Body temperature of the animals was kept in the normal range with a heating pad during and after surgery.

### Cell culture

Mouse cortical neurons were cultured as described previously (Inoue *et al.* 2010, Inoue *et al.* 2012). Pregnant Swiss mice (embryonic day 16) were anesthetized with halothane followed by cervical dislocation. Brains of fetuses were removed rapidly and placed in  $\text{Ca}^{2+}/\text{Mg}^{2+}$ -free cold phosphate-buffered saline. Cerebral cortices were dissected under a dissection microscope and incubated with 0.05% trypsin-EDTA for 10 min at 37°C, followed by trituration with fire-polished glass pipettes. Cells were counted and plated in poly-L-ornithine-coated culture dishes or 24-well plates at a density of  $1 \times 10^6$  cells or  $2 \times 10^5$  cells, respectively. Neurons were cultured with Neurobasal medium (Invitrogen) supplemented with B-27 (Invitrogen) and glutamine, and maintained at 37°C in a humidified 5%  $\text{CO}_2$  atmosphere incubator. Cultures were fed twice a week. Neurons were used for the experiments between days 11 and 16 *in vitro*.

### Quantitative Real-time PCR

Quantitative real-time PCR was performed to validate the expression changes of selected genes SYBR<sup>®</sup> Green supermix (Bio-rad) in C1000<sup>™</sup> Thermal cycler (Bio-rad) in accordance with the manufacturer's protocols. The PCR amplification cycles consisted of denaturation at 95°C for 10 min, 40 cycles of denaturation at 95°C for 5 sec, and annealing/extension at 61°C to for 10 sec, followed by the detection of melt curve, 65°C to 95°C. Real-time PCR reactions were carried out in duplicate or triplicate for each sample and the average values were applied to the  $2^{-\text{Ct}}$  method for data analysis. Relative levels of target mRNA were calculated as  $2^{-\text{Ct}}$ . Primer sets were described in the "Supplementary Table 1".

### Immunoblotting

Immunoblotting was performed as described (Inoue & Xiong 2009). Briefly, cells were lysed in lysis buffer (50 mM Tris-HCl, pH 7.5, 150 mM NaCl, 1% Triton X-100, protease inhibitor and phosphatase inhibitor cocktail). After centrifugation at 13,000g at 4 °C for 10 min, the lysates were collected. The aliquots were mixed with Laemmli sample buffer and

boiled at 95 °C for 10 min. Proteins were separated by 7.5% SDS-PAGE, transferred to PVDF membranes, and probed with antibodies against phospho-Nedd4-2 (phospho-Ser342, 1:1000; Cell Signaling), actin (1:1000; Sigma), and SGK1 (1:200; Abcam) followed by HRP-conjugated secondary antibodies (1:1000). The signals were visualized by chemiluminescence using an ECL kit (Millipore).

### Lactate dehydrogenase (LDH) assay

LDH measurement was performed as described in our previous studies (Inoue *et al.* 2010, Xiong *et al.* 2004). Fifty  $\mu$ l of the culture medium was taken from each well and placed into a 96-well plate for background LDH measurement. Cells were then treated with  $Mg^{2+}$ -free medium in the absence or presence of 100  $\mu$ M NMDA for 1 h, followed by 3 washes and incubation in normal culture medium for 5 h. Fifty  $\mu$ l of the medium was transferred from each well to 96-well plates for measurement of injury-mediated LDH release. For measurement of the maximal releasable LDH, cells were incubated with Triton X-100 (final concentration 0.5%) for 30 min at the end of each experiment. Assay was done with the cytotoxicity detection kit (Roche Diagnostics) according to the manufacturer's instruction.

### Ca<sup>2+</sup> imaging

The intracellular Ca<sup>2+</sup> level of mouse cortical neurons was imaged using Fluo-4 (Invitrogen). Tetrodotoxin (TTX, 0.1  $\mu$ M) and nimodipine (2.5  $\mu$ M) were added in standard extracellular fluid (ECF), which contained (in mM): 140 NaCl, 5.4 KCl, 2 CaCl<sub>2</sub>, 1 MgCl<sub>2</sub>, 10 glucose, and 20 HEPES (pH 7.4 with NaOH, 320–335 mOsm). NMDA (10  $\mu$ M) was applied together with 3  $\mu$ M glycine in  $Mg^{2+}$ -free ECF. Cells were pretreated with DMSO or gsk650394 for more than 5 min before application of NMDA.

### Electrophysiology

Whole-cell patch-clamp recordings were performed as described previously (Inoue *et al.* 2010, Li *et al.* 2014). To evoke NMDA current, 100  $\mu$ M NMDA was applied together with 3  $\mu$ M glycine in  $Mg^{2+}$ -free ECF.

Gramicidin-perforated patch-clamp recording was performed as described previously (Inoue *et al.* 2006, Inoue *et al.* 2012). Gramicidin was dissolved in DMSO and then diluted in the pipette-filling solution to a final concentration of 5–10  $\mu$ g/ml just before the experiment.

### Statistical Analysis

Data are presented as means  $\pm$  SEM. Differences between groups were compared using a one-way ANOVA, paired Student's t-test or unpaired Student's t-test as appropriate. Dunnett's test was used to compensate for multiple experimental procedures.  $p < 0.05$  was regarded as statistically significant.

## Results

### SGK inhibitors reduce infarct volume in mice

We first examined whether the expression of SGK1 changes in our brain ischemia model, since there have been conflicting reports regarding the change of SGK1 expression after

brain ischemia (Nishida *et al.* 2004, Zhang *et al.* 2014). As a result, mRNA and protein levels of SGK1 were not clearly altered (Supplementary Figure 1A and B). The larger band, which may indicate SGK1.1 as suggested by Arteaga *et al.* (Arteaga *et al.* 2008), did not show a clear change either (Supplementary Figure 1B).

Next, to determine whether inhibitors for SGK influence the outcome of ischemic brain injury, we compared the brain damages produced by MCAO in the absence or presence SGK inhibitors in mice (Sherk *et al.* 2008, Ackermann *et al.* 2011). After anesthesia, either vehicle or individual SGK inhibitor was injected into lateral ventricle, and then MCAO was applied for 1 h, followed by reperfusion. Twenty four hours later, the mice were sacrificed and the infarcted size was measured by TTC staining. In mice injected with vehicle, the percentage of infarct volume was  $50.5 \pm 2.2\%$  ( $n=15$ , Figure 1). Contrary to our expectation, the infarct volume in mice injected with SGK inhibitors was significantly smaller (gsk650394;  $30.3 \pm 4.5\%$ ,  $n=10$ ,  $p<0.01$ , EMD638683;  $39.3 \pm 2.9\%$ ,  $n=10$ ,  $p<0.01$ , Figure 1A). We also investigated the effect of SGK inhibition on the infarct volume under diabetic condition, which is one of the common comorbidities of stroke (Janghorbani *et al.* 2007, Soedamah-Muthu *et al.* 2006, Khoury *et al.* 2013). Similar results were observed in type I diabetic mice that underwent 45 min MCAO; administration of gsk650394 significantly decreased the infarct volume (DMSO;  $52.3 \pm 3.3\%$ ,  $n=4$ , gsk650394;  $39.0 \pm 4.2\%$ ,  $n=4$ ,  $p<0.05$ , Figure 1B). Collectively, these data suggest that SGK inhibitors attenuate the stroke-mediated brain injury.

### **SGK inhibitors decrease NMDA toxicity and NMDA-mediated intracellular $\text{Ca}^{2+}$ increase**

To investigate the mechanism by which SGK inhibition ameliorates the insult, *in vitro* neurotoxicity assay was carried out. A previous report has shown that neuronal damage under the condition of oxygen and glucose deprivation is mediated predominantly by NMDA receptors (Aarts *et al.* 2003). Therefore, NMDA was applied to the cells and the LDH release was examined to evaluate neuronal toxicity *in vitro*. When cells were incubated with NMDA, they showed an increase of cell injury as demonstrated by morphological changes (Figure 2A) and increased LDH release measured at 6 h after NMDA application (Figure 2B). The NMDA-induced cell injury was significantly inhibited by both gsk650394 and EMD638683 (Figure 2A and B).

NMDA toxicity is mainly attributable to excessive intracellular  $\text{Ca}^{2+}$  increase (Harukuni & Bhardwaj 2006). To examine whether  $\text{Ca}^{2+}$  permeation mediated by NMDA-Rs is influenced by SGK inhibitor, fluorescence  $\text{Ca}^{2+}$  imaging was carried out using Fluo-4. In the absence of SGK inhibitor, transient application of NMDA generated more than 4-fold increases in fluorescence intensity ( F/F:  $4.46 \pm 0.34$ ,  $n=26$ , Figure 2C). In the presence of gsk650394, fluorescence intensity was only increased ~2-fold ( F/F:  $2.36 \pm 0.13$ ,  $n=32$ ,  $p<0.01$ , Figure 2C and D). Thus, inhibition of SGK ameliorates  $\text{Ca}^{2+}$  increase mediated by NMDA-Rs and these data suggest that SGKs are implicated in neurotoxicity, at least in part, through NMDA-Rs.

### SGK inhibitors attenuate NMDA currents

Next, whole-cell patch-clamp recording was carried out to further examine the effect of SGKs on NMDA-Rs. As shown in Figure 3A and B, application of 30  $\mu$ M gsk650394 for 10 min caused a significant reduction in the amplitude of NMDA-evoked current. This effect was partially recovered after wash out. A similar result was obtained with EMD638683 but the effect was not reversible after 10 min wash out. In contrast, the amplitude of the NMDA current remained stable throughout the recording period with application of the vehicle (DMSO). These results further suggest that protection against NMDA toxicity by SGK inhibitors is due to their suppression of NMDA current.

Notably, while both inhibitors diminished NMDA currents at the concentration of 30  $\mu$ M, they showed little effect on NMDA current at 10  $\mu$ M (before;  $98.4 \pm 2.3\%$  vs 10 min after 10  $\mu$ M gsk650394 application;  $103.2 \pm 5.5\%$ ,  $n=3$ ,  $p>0.05$ ). Considering the possibility that SGKs and/or other soluble components involved in SGK-dependent regulation can be diluted by the pipette solution, conventional whole-cell patch-clamp recording might have minimized the effects of SGK inhibitors. Therefore, gramicidin-perforated patch-clamp recording was applied to avoid dilution of the potential intracellular soluble components (Kyrozis & Reichling 1995). In contrast to whole-cell patch-clamp recordings, 10  $\mu$ M gsk650394 inhibited the currents by  $\sim 60\%$  under perforated patch-clamp recording (before;  $99.2 \pm 3.7\%$  vs 10 min after 10  $\mu$ M gsk650394 application;  $39.7 \pm 8.4\%$ ,  $n=4$ ,  $p<0.01$ , Figure 3C). These data suggest that intracellular soluble molecules are involved in the regulation of NMDA-Rs by SGKs.

### SGK inhibitor attenuates voltage-gated sodium channel (VGSC) currents

Nav1.5, one of VGSCs, is expressed in cardiac cells and known to be activated by SGK1 (van Bemmelen *et al.* 2004). Also, a recent study has shown that neuronal VGSCs are regulated by Nedd4-2 (Laedermann *et al.* 2013). Given that most of the VGSCs have PY motifs, which play crucial roles in binding to Nedd4-2, we speculated that VGSCs are also potential targets of SGKs in brain neurons. Because VGSCs are important for generation of action potential in neurons and that excessive excitation mediated by VGSCs is harmful under injurious conditions (Taylor & Meldrum 1995), we suspect that the activity of Na<sup>+</sup> channels in neurons is modulated by SGK. In this regard, the effect of gsk650394 on VGSC current was examined in cultured mouse cortical neurons. As shown in Figure 4A, membrane depolarizations from  $-80$  mV holding potential generated fast TTX-sensitive inward currents, which is a characteristic of VGSCs. Application of gsk650394 significantly attenuated the amplitude of VGSC currents ( $34.8 \pm 9.3\%$ ,  $n=5$ ,  $p<0.01$ , Figure 4A). In support of this finding, phosphorylation of Nedd4-2 was diminished by administration of gsk650394 ( $68.7 \pm 14.5\%$ ,  $n=5$ ,  $p<0.05$ , Figure 4B). Thus, it is possible that inhibiting the activity of VGSCs, which prevents excessive neuronal excitation (Clare *et al.* 2000), may have contributed to neuroprotection by SGK inhibitor.

## Discussion

In this study, we have demonstrated that inhibition of SGK activity provides alleviation of neuronal injury by stroke insult. This relief is suggested to be mediated, at least partly, by



reduction of NMDA responses and VGSC currents since excess of NMDA-Rs-mediated  $\text{Ca}^{2+}$  flux and VGSC-dependent neuronal excitation lead to progressive neurotoxicity. In parallel to the decrease of those channel activities, phosphorylation of Nedd4-2 was diminished by SGK inhibition. The reduction in Nedd4-2 phosphorylation likely facilitates the binding of Nedd4-2 to VGSCs and possibly NMDA-Rs, resulting in enhanced turnover of these channels (Gautam *et al.* 2013, Laedermann *et al.* 2013).

SGK1 was first identified as a molecule whose expression is induced by glucocorticoid treatment of tumor cells (Webster *et al.* 1993), and is detectable in the brain with other member SGK1.1, SGK2, and SGK3 (Kobayashi *et al.* 1999, Arteaga *et al.* 2008). SGK1 can be induced, not only by serum and glucocorticoid, but also by several factors, which play important roles in homeostatic maintenance (Lang *et al.* 2010).

SGKs phosphorylate downstream substrates and their target sites often correspond to those of Akt/PKB that are likely to support cellular survival (Lang *et al.* 2006a, Manning & Cantley 2007). SGKs are therefore reported to be beneficial for cellular protection. Indeed, Zhang *et al.* have shown the protective effect of SGK1 through enhanced activity of Akt/PKB signals in neurons (Zhang *et al.* 2014). Based on their findings, we initially expected that SGK inhibitors would lead to detrimental effects in the stroke model. However, they surprisingly turned out to attenuate ischemic brain injury (Figure 1). The exact reason for this discrepancy is unclear, but there have been some differences between their study and our current experiments. For example, MCA was occluded for 2 h in rats in their study (Zhang *et al.* 2014) while ours applied 1h transient MCAO in mice. Regarding the differences of species and duration, therapeutic strategy will need to work on a broad spectrum, and detailed research will give more insights into those inquiries. We may also need to consider the difference of genetic approach and the use of SGK inhibitors. Zhang *et al.* applied gene silencing to abrogate the expression of SGK1 (Zhang *et al.* 2014), but SGK2/3 should still be present. In addition, as shown in Supplementary Figure 1B, which is consistent with an earlier study (Arteaga *et al.* 2008), the dominant presence of SGK1.1 is recognized in brain tissues, and the effect of the approach performed by Zhang *et al.* on SGK1.1 is uncertain since downstream targets between SGK1 and SGK1.1 may be different (Arteaga *et al.* 2008). Also, Zhang *et al.* focused on neuronal SGK1 (Zhang *et al.* 2014) whereas SGK inhibitors injected into ventricles in our study influence SGKs in all types of cells including neurons and glia. In line with this, SGK2 and SGK3, but not SGK1, have been reported to facilitate  $\alpha$ -amino-3-hydroxy-5-methyl-4-isoxazolepropionic acid receptor activity (Strutz-Seebohm *et al.* 2005), and SGK3 knockout mice have been shown to express behavioral abnormality (Lang *et al.* 2006b). Thus, isoforms other than SGK1 may also contribute to injury and toxicity shown in Figures 1 and 2. Of note, we cannot rule out the possibility that improved outcome by SGK inhibitors could be due to their effect on blood pressure since one of the SGK inhibitors EMD638683 is reported to lower the blood pressure (Ackermann *et al.* 2011). It has been demonstrated that change in blood pressure influences the outcome of experimental stroke (Hom *et al.* 2007). While this is unlikely, because those inhibitors were injected directly into cerebral ventricles which is less likely affect the blood pressure, we cannot completely exclude the possibility.

## Supplementary Material

Refer to Web version on PubMed Central for supplementary material.

## Acknowledgments

This work was supported by Pilot Research Grant of Center for Excellence of Health Disparity at Morehouse School of Medicine, NIH SC3GM111218 (K.I.), NIH R01NS066027, U54 NS083932 (Z.-G.X.). Institutional support at MSM was provided by NIH/NCRR/RCMI Grant G12RR03034.

## List of abbreviations

<b>SGK</b>	serum- and glucocorticoid-inducible kinase
<b>MCAO</b>	middle cerebral artery occlusion
<b>NMDA</b>	N-methyl-D-aspartate
<b>ENaC</b>	epithelial Na <sup>+</sup> channel
<b>DMSO</b>	dimethylsulfoxide
<b>LDH</b>	lactate dehydrogenase
<b>TTX</b>	tetrodotoxin
<b>ECF</b>	extracellular fluid
<b>VGSC</b>	voltage-gated sodium channel

## References

- Aarts M, Iihara K, Wei WL, Xiong ZG, Arundine M, Cerwinski W, MacDonald JF, Tymianski M. A key role for TRPM7 channels in anoxic neuronal death. *Cell*. 2003; 115:863–877. [PubMed: 14697204]
- Ackermann TF, Boini KM, Beier N, Scholz W, Fuchss T, Lang F. EMD638683, a novel SGK inhibitor with antihypertensive potency. *Cell Physiol Biochem*. 2011; 28:137–146. [PubMed: 21865856]
- Arteaga MF, Coric T, Straub C, Canessa CM. A brain-specific SGK1 splice isoform regulates expression of ASIC1 in neurons. *Proc Nat Acad Sci USA*. 2008; 105:4459–4464. [PubMed: 18334630]
- Benos DJ, Awayda MS, Berdiev BK, Bradford AL, Fuller CM, Senyk O, Ismailov II. Diversity and regulation of amiloride-sensitive Na<sup>+</sup> channels. *Kidney Int*. 1996; 49:1632–1637. [PubMed: 8743467]
- Busjahn A, Aydin A, Uhlmann R, et al. Serum- and glucocorticoid-regulated kinase (SGK1) gene and blood pressure. *Hypertension*. 2002; 40:256–260. [PubMed: 12215463]
- Clare JJ, Tate SN, Nobbs M, Romanos MA. Voltage-gated sodium channels as therapeutic targets. *Drug Discov Today*. 2000; 5:506–520. [PubMed: 11084387]
- Debonneville C, Flores SY, Kamynina E, et al. Phosphorylation of Nedd4-2 by Sgk1 regulates epithelial Na<sup>+</sup> channel cell surface expression. *EMBO J*. 2001; 20:7052–7059. [PubMed: 11742982]
- Federiuk IF, Casey HM, Quinn MJ, Wood MD, Ward WK. Induction of type-1 diabetes mellitus in laboratory rats by use of alloxan: route of administration, pitfalls, and insulin treatment. *Comp Med*. 2004; 54:252–257. [PubMed: 15253270]



- Gautam V, Trinidad JC, Rimerman RA, Costa BM, Burlingame AL, Monaghan DT. Nedd4 is a specific E3 ubiquitin ligase for the NMDA receptor subunit GluN2D. *Neuropharmacology*. 2013; 74:96–107. [PubMed: 23639431]
- Gervitz LM, Nalbant D, Williams SC, Fowler JC. Adenosine-mediated activation of Akt/protein kinase B in the rat hippocampus in vitro and in vivo. *Neurosci Lett*. 2002; 328:175–179. [PubMed: 12133582]
- Gurman P, Miranda OR, Nathan A, Washington C, Rosen Y, Elman NM. Recombinant tissue plasminogen activators (rtPA): a review. *Clin Pharmacol Ther*. 2015; 97:274–285. [PubMed: 25670034]
- Harukuni I, Bhardwaj A. Mechanisms of brain injury after global cerebral ischemia. *Neurol Clin*. 2006; 24:1–21. [PubMed: 16443127]
- Hom S, Fleegal MA, Egleton RD, Campos CR, Hawkins BT, Davis TP. Comparative changes in the blood-brain barrier and cerebral infarction of SHR and WKY rats. *Am J Physiol*. 2007; 292:R1881–R1892.
- Inoue K, Branigan D, Xiong ZG. Zinc-induced neurotoxicity mediated by transient receptor potential melastatin 7 channels. *J Biol Chem*. 2010; 285:7430–7439. [PubMed: 20048154]
- Inoue K, Furukawa T, Kumada T, Yamada J, Wang T, Inoue R, Fukuda A. Taurine inhibits  $K^+$ - $Cl^-$  cotransporter KCC2 to regulate embryonic  $Cl^-$  homeostasis via with-no-lysine (WNK) protein kinase signaling pathway. *J Biol Chem*. 2012; 287:20839–20850. [PubMed: 22544747]
- Inoue K, Xiong ZG. Silencing TRPM7 promotes growth/proliferation and nitric oxide production of vascular endothelial cells via the ERK pathway. *Cardiovasc Res*. 2009; 83:547–557. [PubMed: 19454490]
- Inoue K, Yamada J, Ueno S, Fukuda A. Brain-type creatine kinase activates neuron-specific  $K^+$ - $Cl^-$  co-transporter KCC2. *J Neurochem*. 2006; 96:598–608. [PubMed: 16336223]
- Janghorbani M, Hu FB, Willett WC, Li TY, Manson JE, Logroscino G, Rexrode KM. Prospective study of type 1 and type 2 diabetes and risk of stroke subtypes: the Nurses' Health Study. *Diabet Care*. 2007; 30:1730–1735.
- Khoury JC, Kleindorfer D, Alwell K, et al. Diabetes mellitus: a risk factor for ischemic stroke in a large biracial population. *Stroke*. 2013; 44:1500–1504. [PubMed: 23619130]
- Kobayashi T, Deak M, Morrice N, Cohen P. Characterization of the structure and regulation of two novel isoforms of serum- and glucocorticoid-induced protein kinase. *Biochemical J*. 1999; 344:189–197.
- Kyrozis A, Reichling DB. Perforated-patch recording with gramicidin avoids artifactual changes in intracellular chloride concentration. *J Neurosci Methods*. 1995; 57:27–35. [PubMed: 7540702]
- Laedermann CJ, Cachemaille M, Kirschmann G, et al. Dysregulation of voltage-gated sodium channels by ubiquitin ligase NEDD4-2 in neuropathic pain. *J Clin Invest*. 2013; 123:3002–3013. [PubMed: 23778145]
- Lang F, Bohmer C, Palmada M, Seebohm G, Strutz-Seebohm N, Vallon V. (Patho)physiological significance of the serum- and glucocorticoid-inducible kinase isoforms. *Physiol Rev*. 2006a; 86:1151–1178. [PubMed: 17015487]
- Lang F, Gorlach A, Vallon V. Targeting SGK1 in diabetes. *Exp Opin Ther Targets*. 2009; 13:1303–1311.
- Lang F, Strutz-Seebohm N, Seebohm G, Lang UE. Significance of SGK1 in the regulation of neuronal function. *J Physiol*. 2010; 588:3349–3354. [PubMed: 20530112]
- Lang UE, Wolfer DP, Grahammer F, et al. Reduced locomotion in the serum and glucocorticoid inducible kinase 3 knock out mouse. *Behav Brain Res*. 2006b; 167:75–86. [PubMed: 16246437]
- Li MH, Liu SQ, Inoue K, Lan J, Simon RP, Xiong ZG. Acid-sensing ion channels in mouse olfactory bulb M/T neurons. *J Gen Physiol*. 2014; 143:719–731. [PubMed: 24821964]
- Lo EH, Broderick JP, Moskowitz MA. tPA and proteolysis in the neurovascular unit. *Stroke*. 2004; 35:354–356. [PubMed: 14757877]
- Lu T, Pan Y, Kao SY, Li C, Kohane I, Chan J, Yankner BA. Gene regulation and DNA damage in the ageing human brain. *Nature*. 2004; 429:883–891. [PubMed: 15190254]
- Manning BD, Cantley LC. AKT/PKB signaling: navigating downstream. *Cell*. 2007; 129:1261–1274. [PubMed: 17604717]

- Miyata S, Hattori T, Shimizu S, Ito A, Tohyama M. Disturbance of oligodendrocyte function plays a key role in the pathogenesis of schizophrenia and major depressive disorder. *BioMed Res Int*. 2015; 2015:492367. [PubMed: 25705664]
- Nishida Y, Nagata T, Takahashi Y, Sugahara-Kobayashi M, Murata A, Asai S. Alteration of serum/glucocorticoid regulated kinase-1 (sgk-1) gene expression in rat hippocampus after transient global ischemia. *Mol Brain Res*. 2004; 123:121–125. [PubMed: 15046873]
- Pignataro G, Meller R, Inoue K, Ordonez AN, Ashley MD, Xiong Z, Gala R, Simon RP. In vivo and in vitro characterization of a novel neuroprotective strategy for stroke: ischemic postconditioning. *J Cereb Blood Flow Met*. 2008; 28:232–241.
- Sherk AB, Frigo DE, Schnackenberg CG, et al. Development of a small-molecule serum- and glucocorticoid-regulated kinase-1 antagonist and its evaluation as a prostate cancer therapeutic. *Cancer Res*. 2008; 68:7475–7483. [PubMed: 18794135]
- Slezak M, Korostynski M, Gieryk A, Golda S, Dzbek J, Piechota M, Wlazole E, Bilecki W, Przewlocki R. Astrocytes are a neural target of morphine action via glucocorticoid receptor-dependent signaling. *Glia*. 2013; 61:623–635. [PubMed: 23339081]
- Soedamah-Muthu SS, Fuller JH, Mulnier HE, Raleigh VS, Lawrenson RA, Colhoun HM. High risk of cardiovascular disease in patients with type 1 diabetes in the U.K.: a cohort study using the general practice research database. *Diabetes Care*. 2006; 29:798–804. [PubMed: 16567818]
- Strutz-Seebohm N, Seebohm G, Mack AF, et al. Regulation of GluR1 abundance in murine hippocampal neurones by serum- and glucocorticoid-inducible kinase 3. *J Physiol*. 2005; 565:381–390. [PubMed: 15774536]
- Taylor CP, Meldrum BS. Na<sup>+</sup> channels as targets for neuroprotective drugs. *Trends Pharmacol Sci*. 1995; 16:309–316. [PubMed: 7482996]
- van Bemmelen MX, Rougier JS, Gavillet B, et al. Cardiac voltage-gated sodium channel Nav1.5 is regulated by Nedd4-2 mediated ubiquitination. *Cir Res*. 2004; 95:284–291.
- von Wovern F, Berglund G, Carlson J, Mansson H, Hedblad B, Melander O. Genetic variance of SGK-1 is associated with blood pressure, blood pressure change over time and strength of the insulin-diastolic blood pressure relationship. *Kidney Int*. 2005; 68:2164–2172. [PubMed: 16221215]
- Webster MK, Goya L, Ge Y, Maiyar AC, Firestone GL. Characterization of sgk, a novel member of the serine/threonine protein kinase gene family which is transcriptionally induced by glucocorticoids and serum. *Mol Cell Biol*. 1993; 13:2031–2040. [PubMed: 8455596]
- Wick A, Wick W, Waltenberger J, Weller M, Dichgans J, Schulz JB. Neuroprotection by hypoxic preconditioning requires sequential activation of vascular endothelial growth factor receptor and Akt. *J Neurosci*. 2002; 22:6401–6407. [PubMed: 12151519]
- Wulff P, Vallon V, Huang DY, et al. Impaired renal Na<sup>+</sup> retention in the sgk1-knockout mouse. *J Clin Invest*. 2002; 110:1263–1268. [PubMed: 12417564]
- Xiong ZG, Zhu XM, Chu XP, et al. Neuroprotection in ischemia: blocking calcium-permeable acid-sensing ion channels. *Cell*. 2004; 118:687–698. [PubMed: 15369669]
- Zhang W, Qian C, Li SQ. Protective effect of SGK1 in rat hippocampal neurons subjected to ischemia reperfusion. *Cell Physiol Biochem*. 2014; 34:299–312. [PubMed: 25034177]

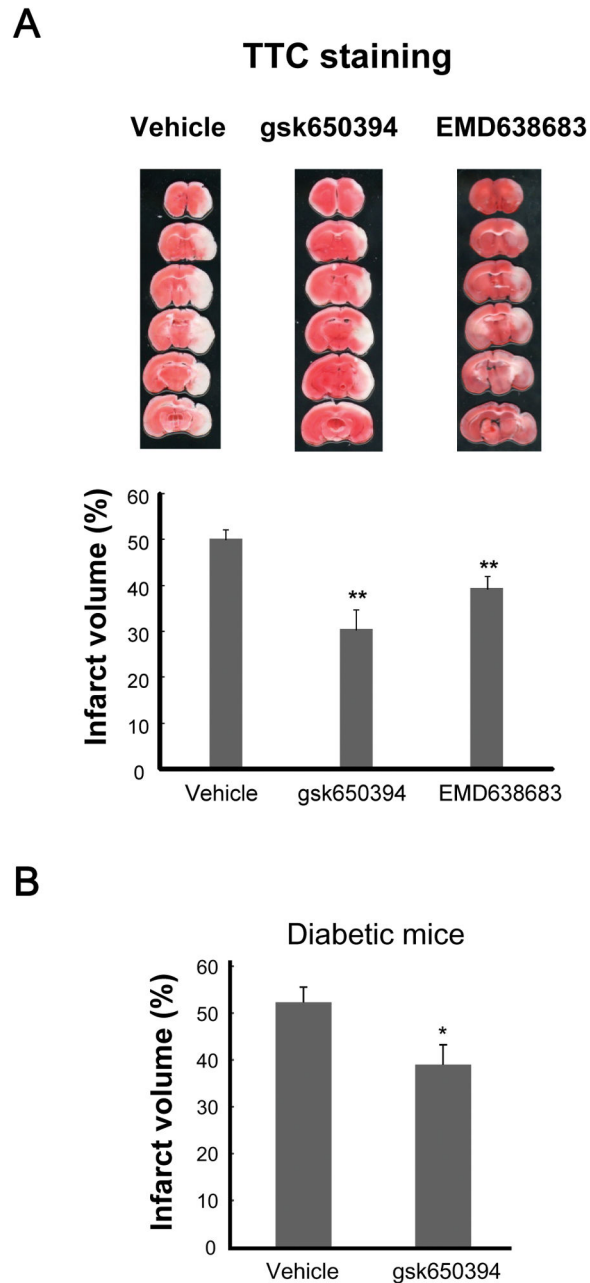


**Figure 1. Neuroprotection by SGK inhibitors in mouse model of brain ischemia**

(A) After injection of vehicle or SGK inhibitor MCAO was carried out for 1 h. Infarct volume was determined 24 h after reperfusion by TTC staining. Representative images of coronal sections stained with TTC staining are shown. Graph shows that the infarct volumes are reduced in the presence of SGK inhibitors. (n=10–15; \*\*p<0.01 vs control, ANOVA followed by Dunnett's test). (B) One week after injection of alloxan, mice were subject to 45 min MCAO, followed by 24-h reperfusion and TTC staining. Graph shows that the infarct volumes are reduced in the presence of gsk650394 (n=4; p<0.05 vs vehicle, unpaired t-test).

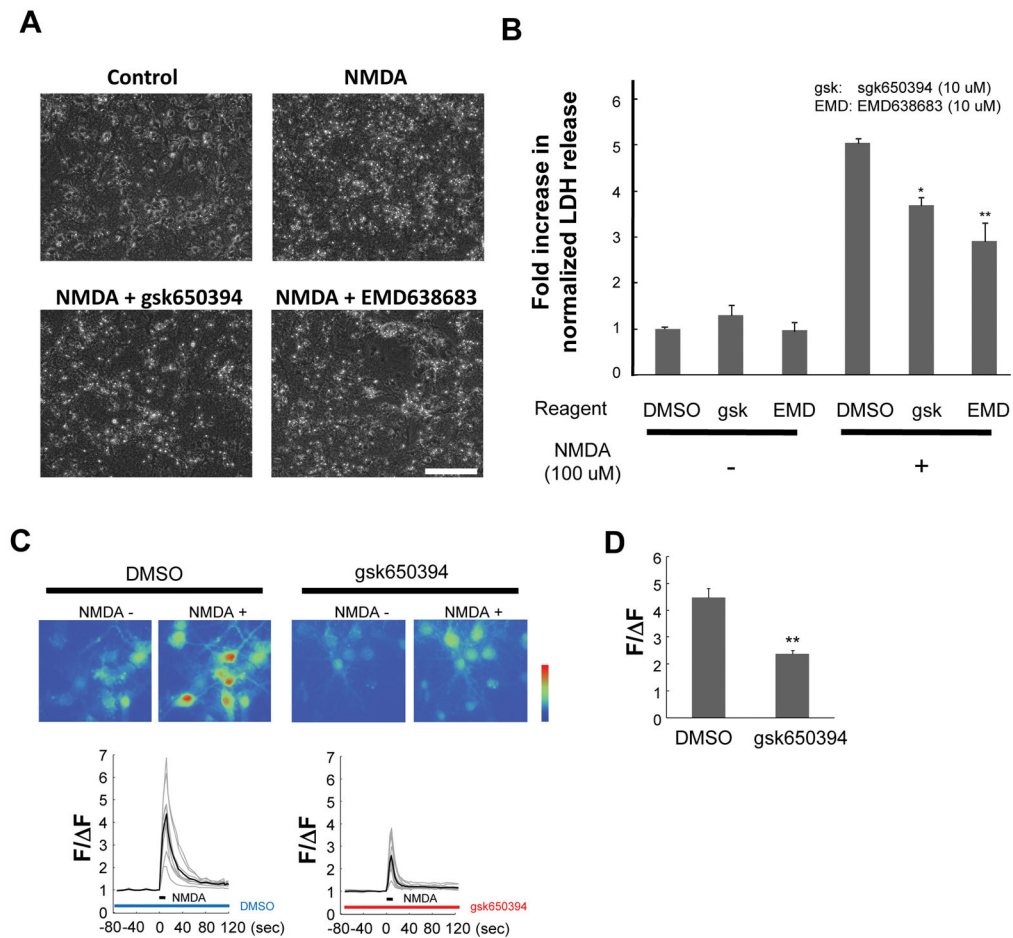


**Figure 2. Attenuation of NMDA-induced neurotoxicity and NMDA-induced Ca<sup>2+</sup> increase by SGK inhibitors**

Cultured mouse cortical neurons were incubated with NMDA in the absence (DMSO) or presence of individual inhibitor for 1 h. Cells were then incubated in growing media for 5 h. (A) Representative phase-contrast images showing cultured cells untreated or treated with NMDA with or without SGK inhibitors. Scale bar; 100  $\mu$ m. (B) Relative LDH release normalized to the maximal values. (n=3; \*p<0.05, \*\*p<0.01 vs DMSO, ANOVA followed by Dunnett's test). (C) Representative images and traces showing NMDA-dependent changes of fluorescence intensity of Fluo-4 in cultured mouse cortical neurons before (left) and after (peak point, right) treatment with SGK inhibitor. Each gray trace represents fluorescent intensity from randomly selected 9–13 cells and black trace stands for an average in an experiment. (D) Summary bar graph showing fold changes in the normalized peak fluorescence intensity in the absence (DMSO) or presence (gsk650394) of SGK inhibitor. n=26–32 cells from three independent experiments (\*\*p<0.01 vs DMSO, unpaired t-test).

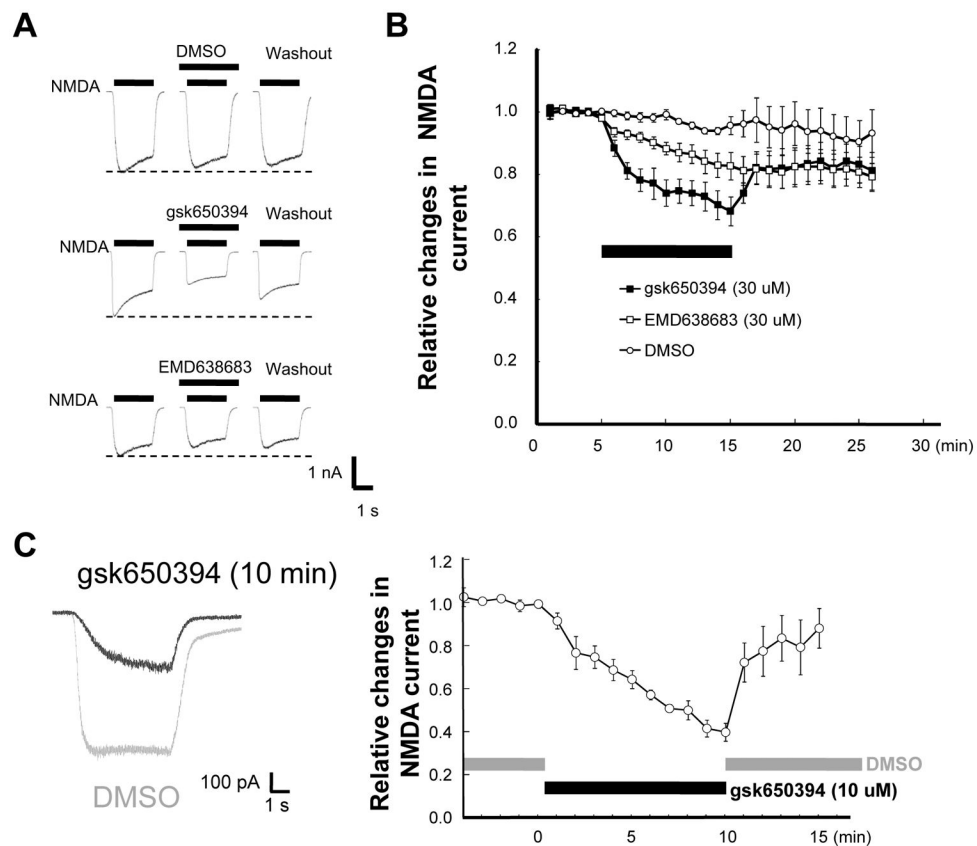


### Figure 3. Inhibition of NMDA-induced current by SGK inhibitors

(A) Representative traces of whole-cell patch-clamp recording showing currents generated by NMDA in cortical neurons in the absence (before) and presence (10 min after treatment) of the indicated inhibitors. (B) Time-dependent changes in normalized peak currents obtained from cells that received different treatments described in (A). (C) Left; representative traces (gray; DMSO, black; 10  $\mu$ M gsk650394) of gramicidin-perforated patch-clamp recording showing currents activated by NMDA in cortical neurons in the absence (gray, before treatment) and presence of SGK inhibitor (black, 10 min after treatment). Right; time-dependent changes in normalized peak currents obtained from cells with gramicidin-perforated patch-clamp recordings.

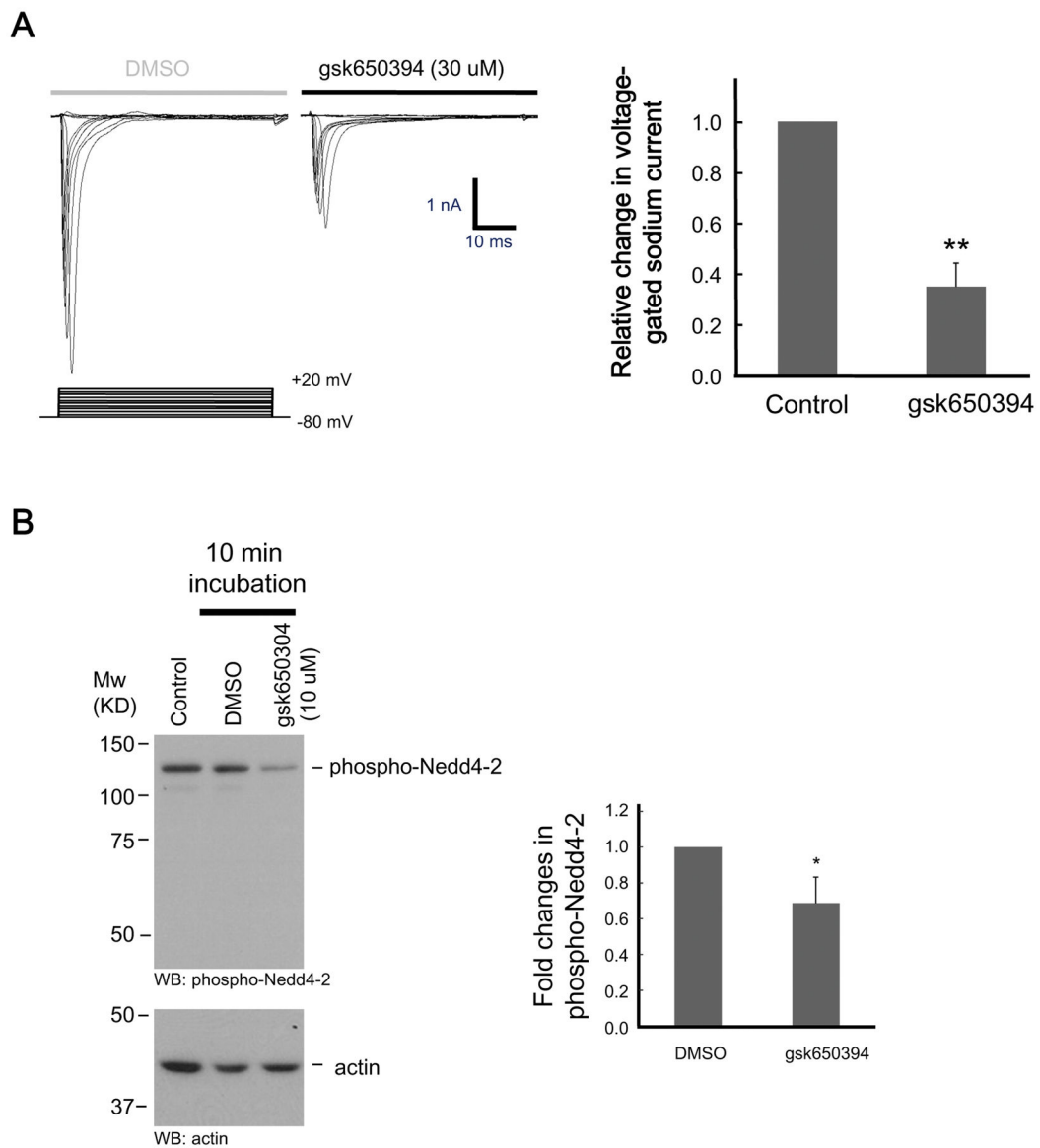


**Figure 4. Attenuation of VGSC currents and phosphorylation of Nedd4-2 by inhibition of SGKs**  
 (A) Representative traces of TTX-sensitive  $\text{Na}^+$  current recorded in cortical neurons before (DMSO) and 10 min after administration of SGK inhibitor (gsk650394). Bar graph shows relative changes in the amplitude of  $\text{Na}^+$  currents before (DMSO) and 10 min after gsk650394 application ( $n=5$ ;  $**p<0.01$  vs DMSO, paired t t-test). (B) Cells were treated with either DMSO or gsk650394 (10  $\mu\text{M}$ ) for 10 min. Cell lysates were then subjected to immunoblotting using an antibody for phospho-Nedd4-2 (upper). Protein loading was monitored using an antibody for actin (lower) ( $n=5$ ;  $*p<0.05$  vs DMSO, unpaired t-test).